

# STRUCTURAL AND FUNCTIONAL IMAGING OF AFFECTIVE DISORDERS

YVETTE I. SHELINE  
MARK A. MINTUN

---

With advances in imaging technology it is now possible to examine subtle changes in both structure and regional function that are associated with the pathophysiology of affective illness. Understanding how these changes fit together with findings from clinical studies, postmortem findings, and animal studies will yield insight into the neuroanatomic pathways involved in affective illness. Combining anatomic MRI studies with functional studies has improved the localization of abnormalities in blood flow, metabolism, and neurotransmitter receptor function and has the potential to provide a better-integrated model of depression. Functional and structural mapping also provide a bridge between the hypotheses stemming from rapidly increasing knowledge of molecular biology, psychopharmacology, and clinical and treatment applications. In this chapter we review studies of structural brain changes associated with early-onset recurrent depression (EORD), late-onset depression (LOD), bipolar disorder, and potential etiologic mechanisms. We also review functional studies in affective illness, including positron emission tomography (PET), functional magnetic resonance imaging (fMRI), and single-photon emission computed tomography (SPECT) studies.

## STRUCTURAL STUDIES

Historically, the major psychiatric illnesses, including affective disorders, were not thought to be associated with structural brain pathology. With the development of new imaging tools in the last two decades, increasing evidence has accumulated that challenges this assumption. Studies using high-resolution three-dimensional (3D) magnetic resonance imaging (MRI) now have a resolution of 1.0 mm or better and are available to examine smaller brain structures with

precision. Initially primarily focused on older subjects, structural studies have found both generalized and localized structural brain changes in major depression and bipolar disorder across the age spectrum.

## Recurrent Unipolar Major Depression

Studies of neuroanatomic structure in early-onset recurrent depression (EORD) have recently found evidence for depression-associated structural change (Table 74.1). Brain changes associated with early-onset major depression have been reported in the hippocampus, amygdala, caudate, putamen, and frontal cortex, structures that are extensively interconnected (20). They comprise a neuroanatomic circuit, which has been termed the limbic–cortical–striatal–pallidal–thalamic (LCSPT) circuit (21). As discussed herein, functional aspects of this circuit are also altered in depression as measured by blood flow and metabolism.

Several studies have examined hippocampal volume in depression. In some (9–12) but not all (13,14,16,17,19) significant reductions in hippocampal volumes were found with depression. In some studies the volume loss appears to have functional significance with an association between acute depression and abnormalities of declarative memory (22) as well as an association between severe depression in remission and lower scores on tests of verbal memory (11). One study (10) found hippocampal atrophy in patients with chronic depression but not in patients with remitted depression. Vakili and colleagues (14) also observed correlations between depression severity and hippocampal volumes, although no group differences between depressed and control subjects.

Methodologic differences may account for some of the discrepancies. The studies reporting negative findings typically had lower resolution, ranging from 3 to 10 mm (6, 14,16,17,19), compared with 0.5 mm to 3 mm (9–12) for studies reporting significant differences. Some studies have reported negative findings for the amygdala–hippocampus complex (16–18), using methodology that does not separate

---

**Yvette I. Sheline:** Department of Psychiatry, Washington University School of Medicine, St. Louis, Missouri.

**Mark A. Mintun:** Department of Radiology, Washington University School of Medicine, St. Louis, Missouri.

**TABLE 74.1. BRAIN STRUCTURAL CHANGES REPORTED IN MAJOR DEPRESSIVE DISORDER<sup>a</sup>**

| Author                          | Brain Region                   | Sample (Number and Diagnosis)  | Age (Mean ± SD)                          | Methods and Resolution                  | Findings  |
|---------------------------------|--------------------------------|--|--|---|---|
| Krishnan et al., 1992 (1)       | Frontal lobe                   | 50 NC<br>50 MDD  | 49.3 ± 18<br>48.3 ± 17                   | 1.5 T<br>5 mm                           | Bifrontal distances smaller<br>Bifrontal brain widths smaller   |
| Coffey et al., 1993 (2)         | Frontal lobe                   | 76 NC<br>48 MDD<br>(44 unipolar;<br>4 bipolar)<br>ECT referred                             | 62.4 ± 16.4<br>61.6 ± 15.9               | 1.5 T<br>5 mm<br>5.2 interval           | Smaller frontal lobe volumes in major depression                |
| Drevets et al., 1997 (3)        | Subgenual prefrontal cortex    | 33 NC<br>13 MDD<br>10 MDD, remitted  | 36.2 ± 8.9<br>33.6 ± 10.0<br>30.1 ± 7.8  | 1.5 T<br>1 mm                           | Smaller subgenual prefrontal cortex volumes in major depression |
| Krishnan et al., 1992 (1)       | Caudate                        | 50 NC<br>50 MDD  | 49.3 ± 18<br>48.3 ± 17                   | 1.5 T<br>5 mm                           | Decreased caudate volumes in major depression                   |
| Greenwald et al., 1997 (4)      | Caudate                        | 30 NC<br>36 MDD  | 72.8 ± 6.6<br>75.9 ± 6.7                 | 1.0 T<br>3 mm                           | Decreased left caudate volume in major depression               |
| Husain et al., 1991 (5)         | Putamen                        | 44 NC<br>41 MDD  | 56.4 ± 19.2<br>55.3 ± 18.8               | 1.5 T<br>5 mm<br>(2 patients with 7 mm) | Decreased putamen volume in major depression                    |
| Dupont et al., 1995 (6)         | Caudate and lenticular nucleus | 26 NC<br>36 MDD-bipolar<br>30 MDD-unipolar   | 39.1 ± 9.4<br>36.6 ± 10.8<br>38.6 ± 10.6 | 1.5 T<br>5 mm–2.5 mm gap                | No significant difference                                       |
| Lenze, Sheline, 1999 (7)        | Caudate and putamen            | 24 NC<br>24 MDD-remitted   | 52.8 ± 17.8<br>52.8 ± 18.4               | 1.5T<br>0.5 mm                          | No significant difference                                       |
| Axelson et al., 1992 (8)        | Pituitary                      | 21 MDD<br>(1 bipolar; 1 adjustment disorder; 1 multi-infarct dementia; 1 schizo affective) | 47.9 ± 18.4<br>39.6 ± 13.2               | 1.0 T<br>3 mm                           | Increase in pituitary volume in major depression                |
| Sheline et al., 1996 (9)        | Hippocampus                    | 10 NC<br>10 MDD, remitted  | 68.0 ± 9.5<br>68.5 ± 10.4                | 1.5 T<br>0.5 mm                         | Decreased hippocampal gray matter volume in major depression    |
| Shah et al., 1998 (10)          | Hippocampus                    | 20 NC<br>20 MDD<br>20 TRD  | 49.3 ± 11.8<br>47.7 ± 9.9<br>48.9 ± 9.8  | 1.0 T<br>2 mm                           | Decreased hippocampal volume in treatment resistant depression  |
| Sheline et al., 1999 (11)       | Hippocampus                    | 24 NC<br>24 MDD-remitted   | 52.8 ± 17.8<br>52.8 ± 18.4               | 1.5 T<br>0.5 mm                         | Decreased hippocampal volume in major depression                |
| Bremner et al., 2000 (12)       | Hippocampus                    | 16 NC<br>16 MDD<br>(1 panic disorder)  | 45.0 ± 10.0<br>43.0 ± 8.0                | 1.5 T<br>3 mm                           | Decreased hippocampal volume in major depression                |
| Mervaala et al., 2000 (13)      | Hippocampus                    | 17 NC<br>34 MDD<br>(6 bipolar, 28 monopolar)   | 42.1 ± 14.6<br>42.2 ± 12.2               | 1.5 T<br>3 mm                           | No significant difference                                       |
| Vakili et al., 2000 (14)        | Hippocampus                    | 20 NC<br>38 MDD  | 40.3 ± 10.4<br>38.5 ± 10.0               | 1.5 T<br>3 mm                           | No significant difference                                       |
| Sheline, Gado, Price, 1998 (15) | Amygdala                       | 20 NC<br>20 MDD, remitted  | 53.8 ± 17.7<br>54.1 ± 18.1               | 1.5 T<br>0.5 mm                         | Decreased amygdala core nuclei volume in major depression       |

(continued)

TABLE 74.1. (continued)

| Author                     | Brain Region                     | Sample (Number and Diagnosis)               | Age (Mean $\pm$ SD)                                | Methods and Resolution               | Findings  |
|----------------------------|----------------------------------|---|--|--------------------------------------|---|
| Bremner et al., 2000 (12)  | Amygdala                         | 16 NC<br>16 MDD<br>(1 panic disorder)       | 45.0 $\pm$ 10.0<br>43.0 $\pm$ 8.0                  | 1.5 T<br>3 mm                        | Increased right amygdala volume in major depression                 |
| Mervaala et al., 2000 (13) | Amygdala                         | 17 NC<br>34 MDD<br>(6 bipolar, 28 unipolar) | 42.1 $\pm$ 14.6<br>42.2 $\pm$ 12.2                 | 1.5 T<br>3 mm                        | Significant asymmetry in amygdalar volume (right smaller than left) |
| Swayze et al., 1992 (16)   | Amygdala/<br>hippocampus complex | 55 Schizophrenic<br>48 MDD-bipolar<br>47 NC | 32.3 $\pm$ 35.4<br>33.4 $\pm$ 34.6                 | 0.5 T<br>1-cm thick slices<br>8 cuts | No significant difference   |
| Axelson et al., 1993 (17)  | Amygdala/<br>hippocampus complex | 30 NC<br>19 MDD                             | 46.7 $\pm$ 20.4<br>56.6 $\pm$ 19.1                 | 1.5 T<br>5 mm                        | No significant difference   |
| Pantel et al., 1997 (18)   | Amygdala/<br>hippocampus complex | 13 NC<br>19 MDD<br>27 AD                    | 68.2 $\pm$ 5.3<br>72.4 $\pm$ 8.8<br>71.9 $\pm$ 8.0 | 1.5 T<br>1.25 mm                     | No significant difference   |
| Ashtari et al., 1999 (19)  | Amygdala/<br>hippocampus complex | 46 NC<br>40 MDD                             | 71.4 $\pm$ 0.3<br>74.3 $\pm$ 6.0                   | 1.0 T<br>3.1 mm                      | No significant difference   |

<sup>a</sup>AD, Alzheimer's disease; MDD, major depressive disorder; NC, normal control; T, tesla; TRD, treatment resistant depression.

the two structures. Clinical selection of subjects may also contribute to different findings. Most of these studies used a mixed group of early-onset and late-onset depression, which may therefore have different contributing etiologies. In some studies (9,11,12) subjects were case control-matched for age and education, whereas in other studies subjects were group-matched or the results were corrected statistically for significant covariates. Some but not all studies excluded subjects with other physical illness or any current or past drug or alcohol abuse. In summary, in most studies that assessed depression severity in unipolar subjects and used high-resolution MRI techniques (Fig. 74.1), depression was associated with hippocampal atrophy, ranging from 8% to 19%. The significance and source of the volume loss has not been demonstrated. It is intriguing that a recent postmortem study (23) has found glial cell loss in the dentate gyrus of the hippocampus as well as in the amygdala in major depression.

Study of the amygdala has yielded inconsistent results with depressed subjects exhibiting an increase in volume in the right amygdala (12), loss of normal asymmetry (13), or reduction in the bilateral core nuclei (15). The amygdala is a difficult structure to measure, because in many areas the "cortical amygdala" merges with surrounding cortex. Particular boundaries selected can vary widely.

A number of studies have found decreased volume of basal ganglia structures in major depression, particularly late-onset depression (1,4,5,24), as further discussed. One study has reported negative findings in caudate and puta-

men in depressed subjects who were otherwise physically healthy (7), a criterion not clearly present in other studies.

Volume reductions in frontal cortex have been reported, ranging from 7% overall reduction in frontal lobe volume in major depression (25) to 48% in the subgenual prefrontal cortex (3). A postmortem study of prefrontal cortex in major depression (26) showed that depressed subjects differed significantly from controls in several prefrontal cortical areas. These included rostral orbitofrontal cortex decreases in cortical thickness, neuronal size decrease, and loss of glial cells in layers II to IV. In caudal orbitofrontal cortex there were reductions in glial cells in layers V to VI and decreases in neuronal sizes. Reductions in glial and neuronal cells throughout all layers as well as reduction in cell size were reported in dorsolateral prefrontal cortex. Glial cell loss in the subgenual region of prefrontal cortex has also been reported in major depression (27). Neuropathologic changes such as these could account for some of the MRI volumetric findings in frontal cortex. The prefrontal cortex is particularly important as a target of monoamine projections. Abnormalities in monoamine receptors, transporters, and second messenger systems (28–32) are reported to occur in major depression. It is also possible that overactivation in one part of the interconnected LCSPT neuroanatomic circuit may lead to over excitation in the other components, resulting in excitotoxic damage. The orbitomedial prefrontal cortex has high concentrations of glucocorticoid receptors, potentially rendering it vulnerable to stress-mediated damage (see the following).

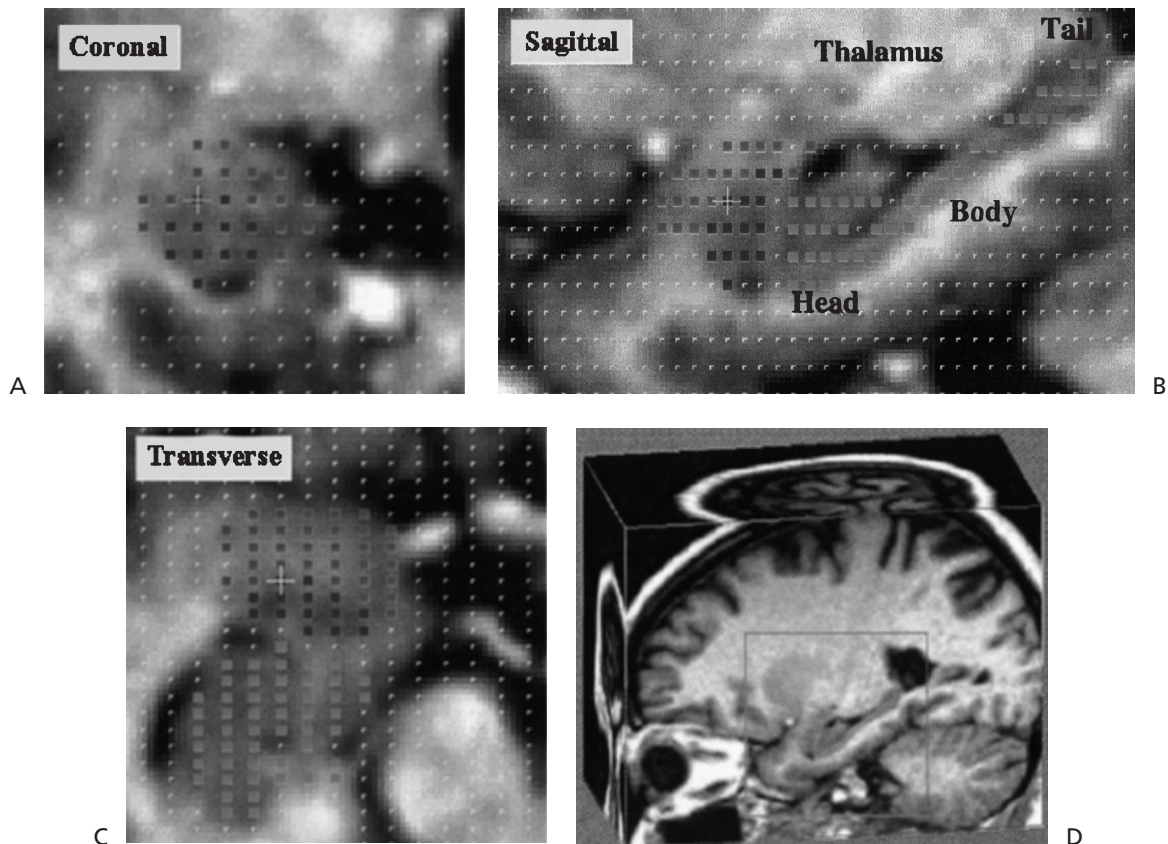


**FIGURE 74.1.** Orthogonal views (coronal, sagittal, and transverse) represent hippocampal and amygdala volumes as they are shown using stereological techniques. A  $5 \times 5 \text{ mm}^2$  grid with a 0.5-mm slice thickness is used to determine volumes for each structure. The total amygdala is made up of green plus blue. Labels for orientation of the hippocampus are included on the sagittal view. These measurements are derived from a cubic subvolume depicted in the last panel.

### Potential Mechanisms for Volume Loss in Early-Onset Recurrent Depression

It has been proposed that hypothalamic–pituitary–adrenal (HPA) axis dysfunction can produce repeated episodes of hypercortisolemia. Currently volume studies do not routinely include measures of cortisol, nor can they ascertain past episodes of hypercortisolemia. However, several different mechanisms could explain volume loss including neuronal loss through exposure to repeated episodes of hypercortisolemia, glial cell loss, resulting in increased vulnerability to glutamate neurotoxicity, stress-induced reduction in neurotrophic factors, and stress-induced reduction in neurogenesis. A mechanism that could account for hippocampal, amygdala, and prefrontal cortex volume loss, areas that have high concentrations of GC receptors is GC-mediated neurotoxicity (33), with repeated hypercortisolemic episodes of depressions giving rise to atrophy. Early life stress may produce a permanent hypersensitivity to stress (34), with the production of ongoing HPA axis dysregulation, particularly in subjects who develop depression. In the case of hippocampal volume loss, the inverse correlations

between the total amount of time patients have been depressed and hippocampal volume (9,11) found in some studies but not all (12) supports recurrent depressive episodes having a causal relationship. Further, a study by Lupien and colleagues (35) demonstrated a correlation between higher cortisol levels measured longitudinally and greater hippocampal volume loss in normal human aging.

Glial cell loss either directly or indirectly is another potential mechanism for producing volume loss. Gray matter atrophy in the prefrontal cortex in an area ventral to the genu of the corpus callosum (3), an area associated in postmortem studies with glial cell loss (27) has been reported. Glial cell loss was also found in another postmortem study of depressed subjects in two different areas of prefrontal cortex (26). In addition, glial cell loss has been reported in postmortem studies of major depression in the amygdala and hippocampus (23).

Through excitatory connections between the amygdala and hippocampus (36) it is possible that damage in one structure could produce damage in the connected structure. Similarly, interconnections between prefrontal cortex and hippocampus (37) could produce excitotoxic damage. Glial

cells sequester glutamate, maintain metabolic and ionic homeostasis, and produce trophic factors, including brain derived neurotrophic factor (BDNF) (38,39). Therefore, loss of glial cells could increase vulnerability to neurotoxic damage, supporting the idea that glutamate neurotoxicity may be involved in the volume loss in the limbic–cortical–striatal–pallidal–thalamic (LCSPT) circuit.

A recently developed concept—stress-induced inhibition of neurogenesis (40)—may also explain depression-related volume loss, although high rates of baseline neurogenesis would be needed to produce atrophy of the scale required by volume loss in depression. Psychosocial stress was shown to suppress neurogenesis in the tree shrew (40). Likewise, corticosterone treatment in adult rats produced suppression of neurogenesis, which was reversed by removal of the adrenal gland (41). More recent findings (42) indicate that neurogenesis may occur in the frontal cortex as well as the hippocampus and subventricular zone. Thus, if depression inhibits neurogenesis, this could potentially explain both cortical and hippocampal volume loss.

### Late-Onset Major Depression

Partly because of the increased prevalence of comorbid illness with age (including cerebrovascular disease, Parkinson's disease, etc.), patients with late life depression have an increased prevalence of structural brain changes relative to EORD. Depression onset in late age frequently occurs in patients with medical and neurologic disorders and compared with EORD it is characterized by greater medical morbidity and mortality (43), higher rates of neuroradiologic abnormalities, particularly white-matter hyperintensities (44,45), and lower familial frequency of affective disorders (46). In some studies, it is associated with higher rates of neuropsychological impairment and treatment refractoriness (47,48).

Both computed tomography (CT) and MRI studies have shown diffuse cortical and subcortical atrophy and ventricular enlargement in late life depression (18,49–51). Specific illnesses that have been associated with brain atrophy include hypertension (52), diabetes (53), Cushing's disease (54), and alcohol abuse (55). Any condition that produces neuronal ischemia or neurotoxicity is a potential candidate for producing brain atrophy.

Neurologic illnesses associated with both cortical and subcortical atrophy are associated with unusually high rates of depression, including Huntington's disease (56), post-stroke syndromes (57), dementia of the Alzheimer's type (58), and Parkinson's disease (59). Each of these illnesses produces damage to brain structures critical in emotional functioning. Importantly, these same brain structures are involved in more classical or early-onset major depression, namely frontal cortex, hippocampus, thalamus, and basal ganglia. Some studies do not find evidence for generalized atrophy in addition to volume loss in structures of the

LCSPT circuit. Kumar and colleagues (60), for example, have found loss in prefrontal lobe volume in late-onset depression in the absence of generalized atrophy, suggesting that as in early-onset depression some subjects with late-onset depression may also have focal volume loss. It is not known whether this focal volume loss involves the same etiologic mechanisms.

A well replicated finding in elderly subject groups with depression is the increased numbers of hyperintensities seen on T2-weighted scans (T2H) (51,61–65). Some studies that included younger subjects with depression have also found increased T2H (2,66), although negative findings have also been reported with younger groups (5,67). The underlying causes of T2H are unknown, and indeed, it is important to note that T2H also occur at rates of up to 60% in healthy elderly (68), in whom their significance is unknown (69). Fujikawa and associates (70,71) found a higher rate of “silent” cerebral infarctions (T2H) in late-compared to early-onset MDD. Clinical correlates of MRI-defined T2H in late-life depression have included older age, vascular risk factors, neuropsychological impairment, and late age of onset (2,48,72). A subtype of “vascular depression” with increased CVD risk factors and increased T2H has been proposed (47,73).

### Bipolar Disorder

Structural abnormalities reported in bipolar disorder have been intermittently reported. These include diffuse gray matter tissue loss, enlarged ventricles, increased numbers of T2-signal hyperintensities (T2H), and regional tissue loss in basal ganglia, lateral and mesial temporal structures, and cortical regions. Studies in bipolar subjects have also found structural changes in the same neuroanatomic circuit (LCSPT) as in major depression but these changes have been less consistent and often involved increases in structure volumes rather than decreases. In addition there is a substantial body of evidence for manic-like affective disorders following focal brain damage.

Most MRI studies have not found generalized cortical gray matter volume loss in bipolar disorder (6,74–78). A recent study in geriatric bipolar disorder (79) found increased cortical sulcal widening which was related to age of illness onset. In a small study in middle-aged bipolar subjects, Lim and co-workers (80) also found enlarged cortical sulci. In the same study, bipolar subjects had generalized decreased cortical gray volume that was intermediate between control and schizophrenia values. This finding could result from differences in segmentation algorithms, differences in covarying the data, and a more chronically ill population. In addition, lateral ventricles were enlarged; however, the difference was not significant in this small sample. Lateral ventricle findings from other groups included increases (45,74,81) and no difference from control (75,82).

Several groups have investigated the question of an over-

all change in temporal lobe volume. Altshuler and colleagues (83) found bilateral temporal lobe reductions comparing bipolar patients to controls. Swayze also found temporal lobe abnormalities in bipolar disorder, but in symmetry rather than in volume—he found that bipolar subjects did not have the usual right greater than left volume asymmetry found in normals (16). In contrast, Harvey and associates (75) found increased left temporal lobe volume in bipolar disorder compared with controls and Johnstone and associates (84) found no differences.

In examining localized structural abnormalities, Strakowski and colleagues examined the circuit comprised of the prefrontal cortex, thalamus, hippocampus, amygdala, globus pallidus, and striatum (LCSPT) and found a significant difference in the overall structural changes. Some of these changes were increases (amygdala, striatum), whereas others were decreases (prefrontal cortex, hippocampus). Others have also examined structural changes in amygdala in bipolar disorder, finding larger (85), smaller (77), or equal (16) volumes. As mentioned, amygdala volumes are difficult to compare between studies. Prefrontal cortex volume decreases (74,76,86) generally have been small but significant in bipolar disorder and are supported by postmortem findings of decreased glia in prefrontal cortex in bipolar subjects (27). Results have been mixed for the basal ganglia. Larger caudate volumes were found in men (87) and larger globus pallidus volumes but not striatal volumes were found in another study (88) in bipolar patients compared to healthy individuals. Other MRI studies did not find any significant differences in bipolar subjects compared to controls in caudate, putamen, or lenticular nuclei (6,16,74). Results have also been mixed for hippocampus (16,85,89) and thalamus (6,74).

A finding that may shed some light in interpreting the contradictory findings is the recent report that chronic lithium treatment is neuroprotective and may prevent volume loss in treated patients (90). Lithium up-regulates the neurotrophic protein Bcl-2 in rat frontal cortex, hippocampus, and striatum. In analyzing reports of volume loss in bipolar patients it may be critical to know the cumulative medication history, especially regarding lithium.

The relationship between bipolar disorder and increased hyperintensities seen on T2-weighted MRI scans (T2H) is complex. The presence of hyperintensities has been associated with hypertension; however, T2H also are increased in asymptomatic elderly. In manic patients who developed bipolar disorder after age 50, Fujikawa and associates (91) found that compared with age- and sex-matched subjects who had developed affective illness prior to age 50 there was a significantly higher incidence of T2H, comparable to the incidence in subjects with late-onset depression. These results are similar to those of McDonald and colleagues (82), who found a higher incidence of subcortical hyperintensities in late-onset bipolar disorder. In younger subjects with new onset bipolar illness Strakowski and colleagues

(74) found a rate of subcortical hyperintensities 1.7 times higher than control subjects, but this was not significant. Aylward and associates (87) also found a higher rate of hyperintensities in bipolar subjects, 34% versus 3% in controls; however, the bipolar subjects were 12 years older on average. In contrast, Figiel and colleagues (45) and Dupont (92) found higher rates of hyperintensities and no age differences. One study did not find differences between bipolar subjects and controls (93).

Most MRS studies have found increased levels of choline-containing molecules in basal ganglia of bipolar subjects compared with controls (94,95); however, Ohara and associates (96) did not find significant differences. Similarly, PET studies have also found functional abnormalities in basal ganglia in bipolar subjects (97,98).

## Conclusion

Although advances in technology have allowed high-resolution studies of individual brain structures, understanding the organization of brain systems has been limited by the lack of noninvasive investigation of neuronal connections between functional regions. The recent development of noninvasive neuronal fiber tracking using water diffusion properties (99) will allow increasingly sophisticated reconstruction of fiber trajectories throughout the brain. The continuing development of automated tissue segmentation methods allowing determination of gray and white matter volumes using computer-generated algorithms will provide faster and more standardized volume measures. It will be important to combine structural studies with functional studies to determine the functional significance of brain structure changes. Combining MRI and functional studies such as PET, SPECT, and fMRI has the potential to more precisely localize abnormalities in blood flow/metabolism, and neurotransmitter receptors. This integrated perspective will allow further development of a structural–functional model of depression.

Studies in high-risk populations, such as first-degree relatives of affected individuals, will assist in determining whether focal structural and functional changes are genetic/neurodevelopmental or acquired and whether they predate or follow the development of depression. Additional postmortem studies in larger samples with careful clinical screening for comorbidity are also needed to examine ultrastructural correlates of volumetric and functional changes. Neuroprotective strategies aimed at preventing the damage associated with depression are likely to be an important future direction for research. Preclinical studies provide preliminary strategies for preventing stress-induced damage. These include for example prevention of stress-induced decreases in brain-derived neurotrophic factor (BDNF) with antidepressants (100–102), prevention of stress-induced excitotoxic injury with phenytoin (Dilantin) (103), prevention of stress-induced decreases in neurogenesis with antide-

pressants (104,105), and increase in dendritic branching with serotonin reuptake inhibitors (106).

## FUNCTIONAL STUDIES

Functional imaging extends the sensitivity and specificity of structural imaging. As it can safely be assumed that genetic, molecular, and biochemical changes precede changes in structure, the promise of functional imaging in affective disorder is to more accurately define the pathophysiology of affective diseases, better predict potential treatments and, in general, further our knowledge of mood regulation by the human brain. Despite its development over a decade ago, functional imaging has only begun to address these primary issues. The principal reason for this slow progress is the need for extensive methodologic development in both major divisions of functional imaging. In the mapping of brain function, the imaging techniques per se have not been a major factor. Rather, the limitation has been in the development and validation of relevant affective “tasks” to selectively activate the brain regions of interest. However, the widespread lack of suitable tracers and probes is the limiting factor in molecular imaging. Sufficiently selective and sensitive probes for the different receptors, enzymes, and transporters that are putatively implicated in affective disorder must be individually developed and validated. Often such probes fail after reaching the level of human application. However, advances in imaging the serotonergic system, for example, have been reported despite these difficulties. It is in this context that we can examine the contribution of functional imaging to our understanding of affective disorder and understand the promise it holds for the future.

### Mapping Brain Function in Affective Disorders

Imaging of regional neuronal activity in affective illness has yielded intriguing, but heterogeneous, findings. Some of the variability in findings may rest in the different methodologies employed and a clear understanding of the limitations of the imaging techniques is important. Cerebral blood flow (CBF) and cerebral metabolic rate of glucose (CMRG) are well accepted as markers of general regional brain activity (107). As such, increased neuronal firing is reliably associated with increased CBF and CMRG allowing the spatial distribution of either CBF or CMRG to serve as a proxy measure for brain activity.

Some early studies of quantitative regional CBF in patients with major depressive disorder studied at rest reported global reductions (108,109). Regional changes have been reported as well with decreased CBF and metabolism in depressed subjects relative to controls in the dorsolateral prefrontal cortex (110,111). However, these regional changes are small (typically 5% to 10%) and are not consis-

tently seen (112). One conclusion from these early studies is that no visually identifiable pattern of CBF or CMRG is associated with depression, even severe depression. This is in contrast to the altered patterns of CBF and CMRG identified for some other diseases, such as Alzheimer’s disease and Huntington’s chorea. For this and other reasons, functional imaging appears to have no current role in the clinical diagnosis or management of affective illness. However, an important role for functional brain mapping in depressive illness is to elucidate the neuroanatomic systems involved with the symptomatology of this disease. One example has been the characterization of decreased activity in the dorsal prefrontal cortices as being related to negative symptoms (111,113). This finding may best be interpreted as representing the relative hypofunction of these systems clinically in some patients with depression because there is much evidence that this brain area plays an active role in working memory and related executive functions.

This last point underscores the nonuniformity of the baseline state as the likely cause of the highly variable results in functional imaging studies of affective illnesses. Different cognitive and emotional states in control subjects are well known to result in regional brain activation. Thus, depressed patients imaged in a “resting” state could have highly variable internal ruminations, emotional states, and cognitive activities. This problem is usually addressed by large sample sizes in most clinical research in which these variations average out; however, as imaging studies are expensive most research studies have been limited to small sample sizes. Combining image data across sites is frustrated by differing instrumentation and approaches to data collection (image resolution, scan timing, etc.). Further complicating imaging studies is the large potential number of regions that can be independently sampled. Only in the last few years have techniques for multiple comparison correction been fully incorporated into data analysis strategies.

Imaging research into altered brain function in affective illnesses does not have to be based solely on a single image, or snapshot. Functional brain imaging of the depressed patient in a single state, a snapshot of brain function, can be complemented by examining the functional changes during a specific task or stimulus (114). The regional brain *responses* to a cognitive or emotional task could be highly informative in understanding the brain during depression. As detailed in Chapter 29, the most sensitive manner in which to demonstrate such brain responses is by comparing two images, on a voxel-by-voxel basis, obtained in two different states in the same individual; effectively subtracting a control image from the test image (115,116). Increased or decreased neuronal activity in the test state will be reflected by increased or decreased CBF in the subtraction image; thus, the pattern of increased activity “maps” the processing areas used by the brain for the task. However, many tasks pertaining to uniquely human activities (e.g., language, declarative memory, emotion) clearly involve numerous brain systems

operating simultaneously and inseparably. Interpretation of a brain-mapping image resulting from such mental activity is problematic. Activated areas assumed to be involved in low-level processing of sensory information (e.g., visual or auditory cortex) may actually contain high-level processing or be critically modulated by other attentional and cognitive processes. Interpretation of brain-mapping studies in which complex tasks are employed require careful use of specific control tasks as opposed to simple “rest” state images. The best control tasks will differ from the task of interest in only the parameter of interest.

Unfortunately, designing tasks suitable for the PET or MRI scanning environment *and* relevant to the major depressive state have been difficult. Important work has been done, however. For example, induction of different emotions via different strategies has been accomplished and demonstrates neuroanatomic systems independent of the induction strategy (117,118). One difficulty with many emotional tasks is that the subject is highly aware of the investigators’ efforts. An alternative to inducing a consciously perceived emotion is to present affect-laden stimuli at an unconscious level (119). This work developed a technique for presenting fearful faces with masking to prevent conscious processing of the visual stimuli. Fearful faces, in contrast to neutral or happy faces, have been reported by multiple investigators to invoke an increase in amygdala activity. By masking the briefly presented (<40 msec) fearful faces with neutral faces, Whalen and colleagues (119) developed a task that isolates the subconscious processing of affect laden stimuli without the confounding variable of individual cognitive processing. Despite the inability of the normal volunteers to report the emotions of the masked faces, amygdala activation was identified with fMRI during the fearful faces presentation. Such paradigm design may prove useful in investigation of affective illnesses such as depression and anxiety disorders.

The application of brain mapping to research in affective disease is still in its infancy because of only recent development of some appropriate task paradigms; however, the area has substantial promise. For example, functional MRI was used to map changes in brain activity in depressed patients and normal controls while viewing a film segment chosen to induce sadness (120). The depressed patients had significantly more activation in areas of the prefrontal cortex. Increased activation in the prefrontal cortex of the depressed cortex could be secondary to increased processing of the stimuli and associated emotions. For many tasks increased prefrontal activation accompanies an increase in task difficulty; however, several issues, including the potential for differences in cognitive response or attention level to the film being shown, must temper the interpretation of this work. Further fMRI work on the processing of emotional stimuli in depressed patients is ongoing and will certainly shed more light on this fascinating area of research.

Some consensus has begun to emerge pointing to abnor-

mal function of specific limbic/paralimbic regions in the depressed patient. Drevets and colleagues (3) detected decreased activity in the subgenual region of the anterior cingulate in a group of depressed bipolar patients compared to controls using an image-wide search of PET measures of CBF. Importantly, the finding replicated with a second group of depressed bipolar patients. The finding was again seen when extended to a group of depressed bipolar using CMRG measures and, then again, when extended to a group of unipolar depressed patients with familial pattern. The authors point out that the subgenual anterior cingulate is heavily interconnected with autonomic structures (including the hypothalamus), ventral striatum, amygdala, and brainstem serotonergic systems; all systems implicated in mood and behavior regulation. Mayberg and associates (121) also detected decreased CMRG in the rostral anterior cingulate of unipolar depressed patients compared to control subjects. The actual center location of this region was approximately 15 mm more dorsal than the subgenual region found by Drevets and colleagues. However, in a highly creative approach, Mayberg and associates (122) examined the regional changes in neural activity with multiple PET scans after improvement of symptoms in depressed patients and compared those to the regional changes in neural activity induced by script-induced sadness in control subjects (see Fig. 74.2). Affective symptom remission was associated with an increased activity within dorsolateral prefrontal cortex, inferior parietal, dorsal anterior cingulate, and posterior cingulate and decreases in ventral limbic and paralimbic sites, including the subgenual anterior cingulate and posterior insula.

The relevance of this particular constellation of brain regions to mood was made more certain by the findings of a similar pattern of regional brain activity, but in the opposite direction, in the normals during induced sadness. Sadness induced increases in a region of the subgenual cingulate and decreases in many of the same dorsal cortical regions. For depressed patients, the increases in dorsal cortical regions may reflect increased cognitive function in the remitted state. The decreases in the subgenual anterior cingulate as symptoms resolve appears more complicated. It is not yet possible to conclude from the data presented in Mayberg and associates (122) that the depressed state reflects an *increased* and abnormal functioning of the subgenual cingulate that returns to baseline during remission. The finding of Drevets and colleagues (3) clearly showing *decreased* metabolism in the subgenual cingulate during a depressive episode needs to be reconciled. One explanation is that the decreased activity is conceivably an actual increase in functional activity that only appears decreased on PET imaging owing to partial volume effects. This region was also reported by Drevets and colleagues to have sizable decreases in volume by MRI, a change known to decrease the measured activity. Nevertheless, the subgenual cortex and adjacent anterior

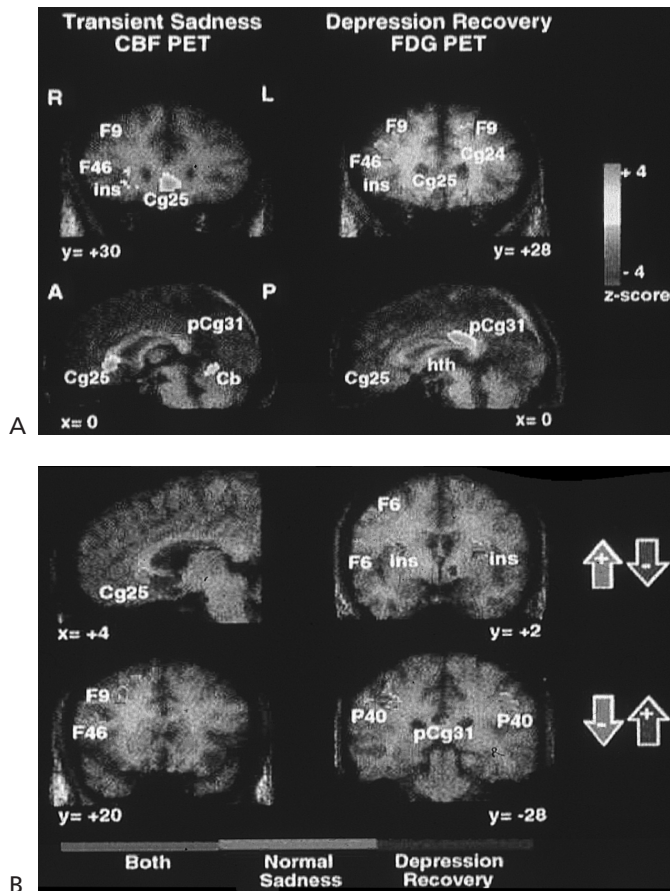


**FIGURE 74.2.** **A:** Left images show changes in regional cerebral blood flow (CBF) (with [ $^{15}\text{O}$ ]water PET) associated with transient sadness in eight healthy volunteers. Right images show changes in regional glucose metabolism (with FDG PET) after six weeks of treatment in eight unipolar depressed patients. Coronal (*top row*) and sagittal (*bottom row*) views. Sadness is associated with increases in ventral paralimbic regions and decreases in dorsal frontal regions. With recovery from depression, the reverse is seen: ventral decreases and dorsal cortical increases. Slice locations are in millimeters relative to the anterior commissure. Numbers are Brodmann area designations. R, right; L, left; A, anterior; P, posterior; F, prefrontal; ins, anterior insula; Cg24, dorsal anterior cingulate; Cg25, subgenual cingulate; pCg, posterior cingulate; Cb, cerebellum; hth, hypothalamus. Color scale: red indicates increases and green indicates decreases in flow or metabolism. **B:** Logical images showing anatomical overlap of significant changes common to both experiments. *Top row:* Concordant areas with increased flow during sadness and decreased metabolism during remission. *Bottom row:* Areas with decreased flow during sadness and increased metabolism during remission. Numbers are Brodmann area designations. F, premotor; p, parietal. Red indicates changes unique to sadness; dark blue indicates changes unique to remission of depression; lighter blue indicates changes common to both. Arrows signify direction of change associated with each condition.

cingulate appear to play an important role in emotional regulation and expression.

### Molecular Imaging of Neurotransmitter Systems in Affective Disorders

Numerous hypotheses have been proposed relating monoamine systems and depression. Serotonin, dopamine, and norepinephrine have all been implicated to various degrees in the behavioral changes and treatment of depression. Of these three, reports indicating a constellation of specific serotonergic dysfunctions in major depressive disorders have been the most convincing. For this reason, much effort in the imaging community has been focused on developing tools for imaging different aspects of the serotonergic system *in vivo*. Generally, these tools have involved the development and validation of radioligands specific for serotonin receptor subtypes (with more than 14 serotonin receptors isolated to date); however, alternative approaches to image serotonergic function have been reported as well. A report by Mann and co-workers (123) demonstrated reduced serotonin responsivity in depressed patients. In that work, fenfluramine, an indirect serotonin agonist, was used as a pharmacologic challenge and FDG PET imaging was used to image the brain responses. Depressed patients showed much less FDG uptake changes in response to fenfluramine than normal controls. Such an approach is limited, however, by the uncertainty in the relationship of the FDG changes and specific aspects of the serotonergic system.

Before reviewing the progress in this rapidly moving field, it is important to note that there is considerable difficulty in synthesizing the literature in both PET and SPECT imaging of receptor function owing to a lack of common data analysis procedures among various imaging groups. As the different data analysis techniques have specific inherent assumptions and limitations, it is useful to briefly review the pertinent issues. For the sake of brevity, we will limit this review to receptor imaging; however, the issues are often identical for imaging of other systems.

Generally, the PET or SPECT imaging device records the brain distribution of a radiotracer that binds selectively at the receptor (or transporter). In many applications a brain region is identified and a time–activity curve for that region is estimated from the images. Multiple factors directly influence the amount of tracer that accumulates in any given brain region: concentration of receptors ( $B_{\max}$ ), dissociation constant between the receptor and ligand ( $K_d$ ), and nonspecific binding to brain tissue (corrected for in some models). In addition, the amount of uptake in the entire brain is dependent on the level of radiotracer in plasma and the degree to which the radiotracer nonspecifically binds to plasma proteins. To measure the  $B_{\max}$  separately from  $K_d$ , the experiment must include some measurements with partial saturation of the receptors; this is rarely done for both logistical and ethical reasons. To address this issue, Mintun and associates (124) proposed a term binding potential (BP)

that combined both terms in the form  $BP = B_{\max}/K_d$ . The binding potential reflects in a single value the ability of the regional brain receptors to bind to free radioligand during equilibrium and, importantly, is linearly related to the  $B_{\max}$ . Thus, if  $K_d$  can be assumed to be constant in the experimental conditions or the different patient populations, the BP can be an adequate substitute for the regional receptor density.

The calculation of BP requires knowledge of the nonspecific binding in plasma and the brain tissue. If the nonspecific binding in plasma is measured or can be assumed, most investigators estimate the nonspecific brain binding of the tracer from a brain region that has negligible amounts of specific binding. A second requirement for calculation of BP is that the kinetics of receptor–ligand interaction be distinguishable from the transport kinetics into the brain. This is true for most tracers, with the receptor binding occurring more slowly than the transport. However, when both processes are of similar rates the BP is difficult to calculate and an alternative term, the distribution volume (DV) has been proposed (125). Conceptually, the DV of a given brain region equals the ratio of brain activity divided by plasma activity at equilibrium and includes the effects of both specific and nonspecific binding. The DV also can be calculated as a parametric image in which each pixel is assigned the appropriate calculated DV value (126). As the DV includes the effect of both specific and nonspecific binding, the DV is usually “corrected” by dividing by the DV of a region where only nonspecific binding occurs. The result, the  $DV_{\text{ratio}}$ , is a frequent form of reporting PET and SPECT receptor data. The use of the  $DV_{\text{ratio}}$  is also applied when the DV values for the areas of interest are not actually calculated from kinetic or equilibrium data, but are estimated from single images. The single image is usually standardized as being at a given time after injection of tracer but may be highly susceptible to individual differences in plasma clearance or transport into the brain.

Further complicating the use of the  $DV_{\text{ratio}}$  is that it is occasionally mistaken as being proportional to  $B_{\max}$  and BP. Actually, the BP is proportional to the term  $DV_{\text{ratio}} - 1$ , which can be substantially different when the  $DV_{\text{ratio}}$  is low. Finally, the calculation of DV and  $DV_{\text{ratio}}$  is usually done without the measurement of plasma binding as it can be shown that the  $DV_{\text{ratio}}$  is mathematically independent of plasma binding. Indeed, the BP differs from the  $DV_{\text{ratio}} - 1$  only by the incorporation of the plasma binding into the BP. Thus, if plasma binding is unknown the use of  $DV_{\text{ratio}} - 1$  is quite appropriate and will remove all individual and group effects of plasma binding in the receptor data. What is usually not appreciated is that individual variations in *brain* nonspecific binding are *not* corrected in the  $DV_{\text{ratio}} - 1$  calculation. This limitation of the  $DV_{\text{ratio}} - 1$  term is rarely discussed and even more rarely quantitatively examined.

The lack of suitable radioligands for human PET imag-

ing has significantly slowed research in affective disorders. The serotonin receptor subtypes with the highest brain densities, 5-HT<sub>1A</sub> and 5-HT<sub>2A</sub> receptors, do have PET radioligands with sufficient selectivity and affinity suitable for imaging (Fig. 74.3). In the 5-HT<sub>2A</sub> system some initial work in depression was done using tracers with limited selectivity. Labeled spiperone (127) demonstrated alterations in binding in depressed post-stroke patients but interpretation must be limited owing to the very high affinity of this tracer for dopamine-2 receptors. 2-<sup>123</sup>I-ketanserin demonstrated increased binding in the right parietal cortex of depressed patients (128), but again, the work is limited by the nonselectivity of ketanserin. Since these initial reports, methodologic development to image 5-HT<sub>2A</sub> receptors has been successful using highly selective agents including [<sup>18</sup>F]altanserin (129), [<sup>18</sup>F]setoperone (130) and labeled MDL100,907 (131,132).

The application of these radioligand techniques in mood disorders has begun with some interesting results. Biver and associates (29) found apparent decreased [<sup>18</sup>F]altanserin binding in the right insular and adjacent orbital cortices in eight medication-free depressed patients. However, as the data processing approach normalized for global [<sup>18</sup>F]altanserin uptake the method cannot distinguish between a true decrease and an increase that is proportionally less than the [<sup>18</sup>F]altanserin binding in the remaining brain. Nonetheless, the detection of a regional change in [<sup>18</sup>F]altanserin binding suggests some type of regional difference in receptor density. Several other studies, however, have not shown altered radioligand binding to 5-HT<sub>2A</sub> receptors during depression. Meyer and co-workers (133) used [<sup>18</sup>F]setoperone to compare 14 medication-free depressed patients with 19 control subjects and found no difference in binding in a large prefrontal cortex region of interest. The data was reported as  $DV_{\text{ratio}}$  and quantitation using plasma activity was not done. Interestingly, the prefrontal cortex value was 1.6 in the depressed group and 1.8 in the control group. After correction of the  $DV_{\text{ratio}}$  to yield a term proportional to receptor density (the BP is proportional to  $DV_{\text{ratio}} - 1$ ) this trend represents a rather large 25% decrease in the depressed group.

Yatham and colleagues (134) used [<sup>18</sup>F]setoperone to measure 5-HT<sub>2A</sub> binding in 20 depressed and 20 controls. All images were first normalized by cerebellar activity to account for differences in nonspecific uptake and then processed using statistical parametric mapping (SPM). Unfortunately, the actual DV image was not calculated, nor the  $DV_{\text{ratio}}$ , as only raw PET activity from a single time frame was used. SPM performed a pixel-by-pixel ANCOVA to detect pixels with significant group differences and showed generalized decreased binding in the frontal and parietal cortices of the depressed patient group. Yatham and colleagues reported that in some voxels the decrease in uptake was 20% to 27%. As the study was done without an equilibrium state or kinetic analysis, it is unknown whether trans-

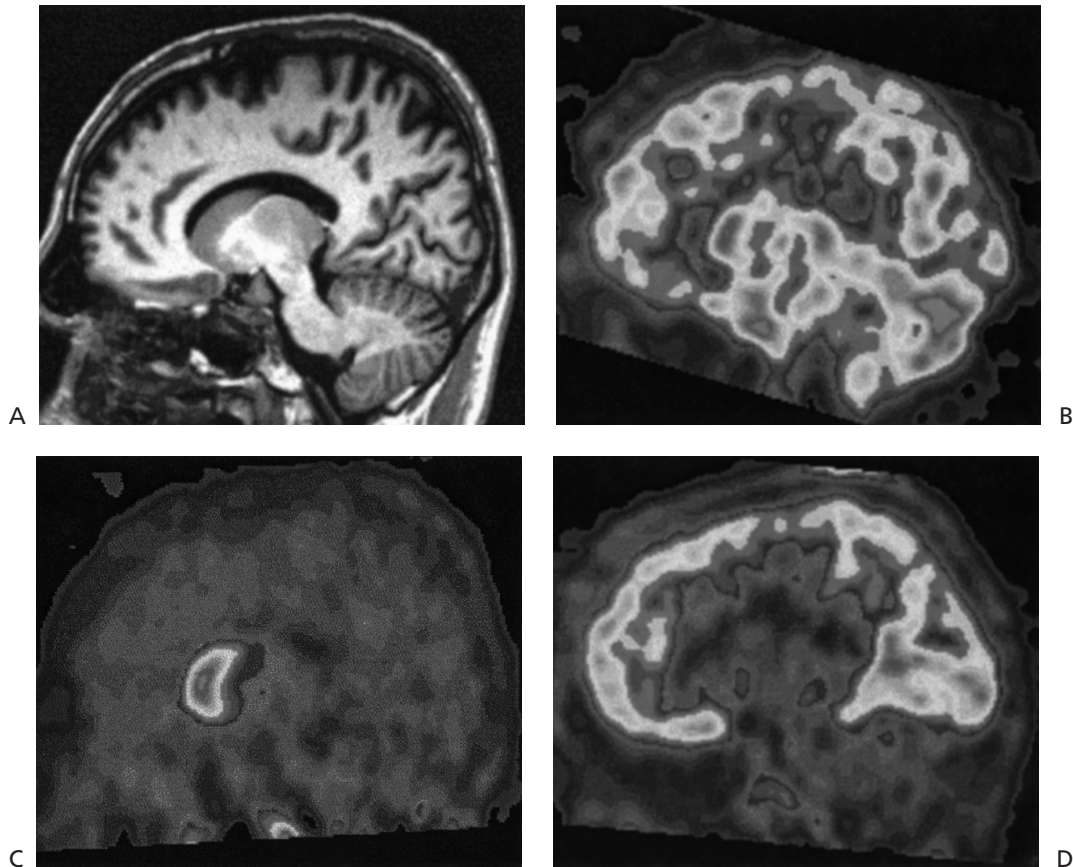


**FIGURE 74.3.** Parasagittal views through the head of the caudate of an anatomic magnetic resonance imaging scan and three different types of functional positron emission tomography scans. All images were collected in normal control subjects and have been converted to a standard atlas coordinate system using linear affine transformation. The upper right image is from a 60-second scan after injection with [ $^{15}\text{O}$ ]water and represents the distribution of cerebral blood flow (CBF). The lower left image is from a 30-minute scan obtained 30 minutes after injection of [ $^{11}\text{C}$ ]raclopride. The scan shows widespread low nonspecific binding (e.g., cerebellum) and focal increased specific binding to  $\text{D}_2$  dopamine receptors in the caudate. The lower right image is from a 30-minute scan obtained 60 minutes after injection of [ $^{18}\text{F}$ ]altanserin. Again, the cerebellum shows low nonspecific uptake, whereas the cortical gray matter shows the specific binding to the  $5\text{-HT}_{2\text{A}}$  serotonin receptors. These images demonstrate the ability to visualize distinct aspects of brain function using different radiotracers. Relatively high CBF is seen throughout the cerebellum and cortical and subcortical gray matter. In contrast,  $\text{D}_2$  receptors are seen to be highly concentrated in the caudate, whereas  $5\text{-HT}_{2\text{A}}$  receptors are concentrated in the cortical gray matter with only small amount of receptor binding in basal ganglia. With the appropriate quantitative processing, these differences in radiotracer uptake can be expressed as relative or absolute receptor density.

port issues could be responsible for some of these results. In another study, Attar-Levy and associates (135) used [ $^{18}\text{F}$ ]setoperone to measure  $5\text{-HT}_{2\text{A}}$  binding in seven depressed patients and seven age-matched controls. Regions of interest over multiple cortical areas were used to measure radioligand uptake at a given time after injection and the data were normalized by first subtracting cerebellar activity and then dividing by injected dose. This result is a non-standard term that is not corrected for variations in plasma nonspecific binding (but may be corrected for variations in brain nonspecific binding). There was little difference

between depressed and control values with only the frontal region demonstrating a significant decrease in bindings (approximately 6%). However, most of the patients were concurrently being treated with benzodiazepines (six of seven), which may have further confounded the results. Finally, Meltzer and colleagues (136) used [ $^{18}\text{F}$ ]altanserin to image eleven late-life depressed patients and age-matched controls. Logan graphical analysis was used to analyze regional activity data and quantitate DV and the  $\text{DV}_{\text{ratio}} - 1$ . Meltzer and colleagues reported no difference between the depressed and control groups.

The preceding data have the common thread that regional measures of 5-HT<sub>2A</sub> binding appear to yield slight, nonsignificant decreases in depressed populations compared to controls. The image-wide processing methods using SPM, which had different methods of normalizing the radioligand uptake data, appeared to yield more dramatic decreases in the depressed populations. As these parametric methods are not well validated with these radiotracers, the significance of the findings will be uncertain until further work, likely using conventional analyses, is done.

The 5-HT<sub>1A</sub> receptor distribution has been imaged in humans using the high-affinity antagonist [<sup>11</sup>C]WAY 100,635 (137,138). The images are unusual because of the very high ratio of specific to nonspecific binding in the brain. Compared to images from labeled setoperone or altanserin, in which approximately one-half of all of the brain activity is not bound to the receptor of interest, the [<sup>11</sup>C]WAY 100,635 PET images have less than 10% of the activity in nonspecific binding and 90% specific activity. The ratio of receptor-rich brain regions to the cerebellum, assumed to be devoid of 5-HT<sub>1A</sub> receptors, is typically greater than 15, depending on the timing of the scan (compared to a ratio of 2 to 3 for altanserin or setoperone). This very high "target-to-background" allows the imaging and even quantitation of 5-HT<sub>1A</sub> receptor content in very small structures, such as the midbrain raphe. Early reports show that 5-HT<sub>1A</sub> receptor binding of [<sup>11</sup>C]WAY 100,635 in a variety of cortical regions and in the raphe is decreased in depressed patients compared to controls (139,140). The observed decreases are substantial, ranging from 20% to 40% in some regions. As 5-HT<sub>1A</sub> receptors are involved in widespread modulation of function in limbic and paralimbic regions, these findings are of considerable importance. Furthermore, the 5-HT<sub>1A</sub> receptors are part of the autoregulation of serotonergic innervation in the raphe, increasing the significance of these findings.

Work on imaging serotonin reuptake sites, the target of the most commonly used antidepressants, is ongoing. The radioligand that has undergone the most study is [<sup>11</sup>C]McNeil 5652. However, nonspecific binding with this tracer is high, and separating the receptor binding from nonspecific binding has been challenging (141,142). One alternative tracer is [<sup>123</sup>I]B-CIT SPECT imaging. This tracer binds to other reuptake sites but has simpler kinetics and can be used in brain regions that have predominantly serotonin reuptake binding. This property was exploited in a study by Malison and co-workers of unipolar, unmedicated depressed patients in which brainstem serotonin reuptake site binding was significantly reduced by nearly 20% compared to controls (143). Another area of interest is in the *in vivo* measure of serotonin synthesis. This has been achieved using  $\alpha$ -<sup>11</sup>C-methyl-tryptophan (144). The tracer is converted to  $\alpha$ -<sup>11</sup>C-methyl-serotonin within neurons and then accumulates, unable to be degraded by monoamine oxidases. The rate of accumulation is argued to be proportional

to endogenous serotonin synthesis (144). However, validation is problematic because there are few tools for verifying rates of serotonin synthesis. Also, it has been noted that the synthetic rates appear to be highly dependent on plasma tryptophan levels.

Dopaminergic innervation in depression may be altered. D'haenen and Bossuyt (145) imaged 23 depressed patients and 11 controls using SPECT and <sup>123</sup>I-iodobenzamide (IBZM), a high-affinity ligand for the D<sub>2</sub> receptor. The activity in the basal ganglia after normalizing with cerebellar activity was 10% greater in the depressed subjects ( $p < 0.025$ ). The authors suggest that this increase reflects decreased dopaminergic neurotransmission. Decreased synaptic dopamine could then result in decreased occupancy of the D<sub>2</sub> receptors and D<sub>2</sub> up-regulation, both factors could lead to increased IBZM binding. In two other reports the IBZM uptake in the striatum was shown to decrease during treatment with antidepressants (146,147), although decreased D<sub>2</sub> receptor binding at baseline in depression was not seen. However, the striatal dopamine system may not be the most critical in affective disorders. With the advent of radioligands able to image extrasynaptic D<sub>2</sub> receptors (e.g., [<sup>18</sup>F]fallypride) (148), investigation of dopaminergic function in limbic cortical regions will be possible.

## Conclusion

The last decade has produced numerous advances in our ability to image brain function. Although the application to affective disorders has been limited to date, the data are tantalizing. Findings have identified abnormalities in the function of limbic cortical structures and the location of these structures overlap with those areas involved with generation of emotion. With increasing sophistication of emotional paradigms, a more precise picture of the role these structures play in mood regulation may emerge. Serotonergic alterations are being further identified with existing techniques and new radioligands will be introduced over the next decade that will greatly expand our imaging capabilities. Novel methods will be explored, leading to agents able to image aspects of gene expression, perhaps even with the spatial and temporal resolution of MRI (149).

## ACKNOWLEDGMENT

Yvette I. Sheline was supported in part by MH01370 and MH58444.

## REFERENCES

1. Krishnan KR, McDonald W, Escalona P, et al. MRI of the caudate nuclei in depression. *Arch Gen Psychiatry* 1992;49: 553-557.
2. Coffey CE, Wilkinson WE, Weiner RD, et al. Quantitative

- cerebral anatomy in depression: a controlled magnetic resonance imaging study. *Arch Gen Psychiatry* 1993;50:7–16.
3. Drevets WC, Price JL, Simpson JR Jr, et al. Subgenual prefrontal cortex abnormalities in mood disorders. *Nature* 1997;386:824–827.
  4. Greenwald BS, Kramer-Ginsberg E, Bogerts B, et al. Qualitative magnetic resonance imaging findings in geriatric depression. Possible link between later-onset depression and Alzheimer's disease? *Psychol Med* 1997;27:421–431.
  5. Husain MM, McDonald WM, Doraiswamy PM, et al. A magnetic resonance imaging study of putamen nuclei in major depression. *Psychiatry Res* 1991;40:95–99.
  6. Dupont RM, Jernigan TL, Heindel W, et al. Magnetic resonance imaging and mood disorders. Localization of white matter and other subcortical abnormalities. *Arch Gen Psychiatry* 1995;52:747–755.
  7. Lenze E, Sheline Y. Absence of striatal volume differences between healthy depressed subjects and matched comparisons. *Am J Psychiatry* 1999;156(12):1989–1991.
  8. Axelson DS, Doraiswamy PM, Boyko OB, et al. In vivo assessment of pituitary volume with magnetic resonance imaging and systematic stereology: relationship to dexamethasone suppression test results in patients. *Psychiatry Res* 1992;44:63–70.
  9. Sheline Y, Wang P, Gado M, et al. Hippocampal atrophy in recurrent major depression. *Proc Natl Acad Sci USA* 1996;93:3908–3913.
  10. Shah PJ, Ebmeier KP, Glabus MF, et al. Cortical grey matter reductions associated with treatment resistant chronic unipolar depression. Controlled magnetic resonance imaging study. *Br J Psychiatry* 1998;172:527–532.
  11. Sheline Y, Sanghavi M, Mintun M, et al. Depression duration but not age predicts hippocampal volume loss in women with recurrent major depression. *J Neurosci* 1999;19:5034–504.
  12. Bremner JD, Narayan M, Anderson ER, et al. Hippocampal volume reduction in major depression. *Am J Psychiatry* 2000;157:115–118.
  13. Mervaala E, Fohr J, Kononen M, et al. Quantitative MRI of the hippocampus and amygdala in severe depression. *Psychol Med* 2000;30:117–125.
  14. Vakili K, Pillay SS, Lafer B, et al. volume in primary unipolar depression: a magnetic resonance imaging study. *Biol Psychiatry* 2000;47:1087–1090.
  15. Sheline YI, Gado MH, Price JL. Amygdala core nuclei volumes are decreased in recurrent major depression. *Neuroreport* 1998;9:2023–2028.
  16. Swayze VW, Andreasen NC, Alliger RJ, et al. Subcortical and temporal structures in affective disorder and schizophrenia: a magnetic resonance imaging study. *Biol Psychiatry* 1992;31:221–240.
  17. Axelson DS, Doraiswamy PM, McDonald WM, et al. Hypercortisolemia and hippocampal changes in depression. *Psychiatry Res* 1993;47:163–173.
  18. Pantel J, Schroder J, Essig M, et al. Quantitative magnetic resonance imaging in geriatric depression and primary degenerative dementia. *J Affect Disord* 1997;42:69–83.
  19. Ashtari M, Greenwald BS, Kramer-Ginsberg E, et al. Hippocampal/amygdala volumes in geriatric depression. *Psychol Med* 1999;29:629–638.
  20. Price J, Russchen F, Amaral D. The limbic region. II: The amygdaloid complex. In: Bjorkland A, Hokfelt T, Swanson L, eds. *Handbook of chemical neuroanatomy*, vol 5. New York: Elsevier, 1987:279–388.
  21. Swerdlow NR, Koob GF. Dopamine, schizophrenia, mania and depression: toward a unified hypothesis of cortico-striato-pallido-thalamic function. *Behav Brain Sci* 1987;10:197–245.
  22. Burt DB, Zembar MJ, Niederehe G. Depression and memory impairment: a meta-analysis of the association, its pattern, and specificity. *Psychol Bull* 1995;117:285–305.
  23. Bowley MP, Drevets WC, Ongur D, et al. Glial changes in the amygdala and entorhinal cortex in mood disorders. *Soc Neurosci Abst* 2000;26:876.
  24. Steffens DC, Krishnan KR. Structural neuroimaging and mood disorders: recent findings, implications for classification, and future directions. *Biol Psychiatry* 1998;43:705–712.
  25. Coffey CE, Wilkinson WE, Parashos IA, et al. Quantitative cerebral anatomy of the aging human brain: a cross-sectional study using magnetic resonance imaging. *Neurology* 1992;42:527–536.
  26. Rajkowska G, Miguel-Hidalgo JJ, Wei J, et al. Morphometric evidence for neuronal and glial prefrontal cell pathology in major depression. *Biol Psychiatry* 1999;45:1085–1098.
  27. Ongur D, Drevets WC, Price JL. Glial reduction in the subgenual prefrontal cortex in mood disorders. *Proc Natl Acad Sci USA* 1998;95:13290–13295.
  28. Arango V, Underwood MD, Gubbi AV, et al. Localized alterations in pre- and postsynaptic serotonin binding sites in the ventrolateral prefrontal cortex of suicide victims. *Brain Res* 1995;688:121–133.
  29. Biver F, Wikler D, Lotstra F, et al. Serotonin 5-HT<sub>2</sub> receptor imaging in major depression: focal changes in orbito-insular cortex. *Br J Psychiatry* 1997;171:444–448.
  30. Mintun MA, Sheline YI, Moerlein SM. Regional [<sup>18</sup>F]altanserin binding in the treatment of major depression. *Neuroimage* 2000;11:S83.
  31. Price JL. Prefrontal cortical networks related to visceral function and mood. *Ann NY Acad Sci* 1999;877:383–396.
  32. Duman RS. Novel therapeutic approaches beyond the serotonin receptor. *Biol Psychiatry* 1998;44:324–335.
  33. Sapolsky RM. Glucocorticoids and hippocampal atrophy in neuropsychiatric disorders. *Arch Gen Psychiatry* 2000;57:925–935.
  34. Heim C, Ehler U, Hellhammer DH. The potential role of hypocortisolism in the pathophysiology of stress-related bodily disorders. *Psychoneuroendocrinology* 2000;25:1–35.
  35. Lupien SJ, de Leon M, deSanti S, et al. Cortisol levels during human aging predict hippocampal atrophy and memory deficits. *Nat Neurosci* 1998;1:69–73.
  36. White LE, Price JL. The functional anatomy of limbic status epileptics in the rat. II. The effects of focal deactivation. *J Neurosci* 1994;13:4810–4830.
  37. Carmichael ST, Price JL. Limbic connections of the orbital and medial prefrontal cortex in macaque monkeys. *J Comp Neurol* 1995;363:615–641.
  38. Szatkowski M, Attwell D. Triggering and execution of neuronal death in brain ischemia: two phases of glutamate release by different mechanisms. *Trends Neurosci* 1994;17:359–365.
  39. Ransom BR, Sontheimer H. The neurophysiology of glial cells. *J Clin Neurophysiology* 1992;9:224–251.
  40. Gould E, McEwen BS, Tanapat P, et al. Neurogenesis in the dentate gyrus of the adult tree shrew is regulated by psychosocial stress and NMDA receptor activation. *J Neurosci* 1997;17:2492–2498.
  41. Cameron HA, Gould E. Adult neurogenesis is regulated by adrenal steroids in the dentate gyrus. *Neuroscience* 1994;61:203–209.
  42. Gould E, Reeves AJ, Graziano MS, et al. Neurogenesis in the neocortex of adult primates. *Science* 1999;286:548–552.
  43. Jacoby RJ, Levy R, Bird JM. Computed tomography and the outcome of affective disorder: A follow-up study of elderly patients. *Br J Psychiatry* 1981;139:288–292.
  44. Coffey C, Figiel G, Djang W. Leukoencephalopathy in elderly

- depressed patients referred for ECT. *Biol Psychiatry* 1988;24:143–161.
45. Figiel GS, Krishnan KRR, et al. Subcortical hyperintensities on brain Magnetic Resonance Imaging: a comparison between late age onset and early-onset elderly depressed subjects. *Neurobiol Aging* 1991;26:245–247.
  46. Baron M, Mendlewicz J, Klotz J. Age-of-onset and genetic transmission in affective disorders. *Acta Psychiatr Scand* 1981;64:373–380.
  47. Alexopoulos GS, Meyers B, Young R, et al. Recovery in geriatric depression. *Arch Gen Psychiatry* 1996;53:305–312.
  48. Simpson S, Baldwin RC, Jackson A, et al. Is subcortical disease associated with a poor response to antidepressants? Neurological, neuropsychological and neuroradiological findings in late-life depression. *Psychol Med* 1998;28:1015–1026.
  49. Soares JC, Mann JJ. The anatomy of mood disorders: review of structural neuroimaging studies. *Biol Psychiatry* 1997;41:86–106.
  50. Rothschild AJ, Benes F, Hebben N, et al. Relationships between brain CT scan findings and cortisol in psychotic and nonpsychotic depressed patients. *Biol Psychiatry* 1989;26:565–575.
  51. Rabins PV, Pearlson GD, Aylward E, et al. Cortical magnetic resonance imaging changes in elderly inpatients with major depression. *Am J Psychiatry* 1991;148:617–620.
  52. Kobayashi S, Okada K, Yamashita K. Incidence of silent lacunar lesion in normal adults and its relation to cerebral blood flow and risk factors. *Stroke* 1991;22:1379–1383.
  53. Aronson S. Intracranial vascular lesions in patients with diabetes mellitus. *J Neuropathol Exp Neurol* 1973;32:183–196.
  54. Starkman MN, Gebariski SS, Berent S, et al. Hippocampal formation volume, memory dysfunction, and cortisol levels in patients with Cushing's syndrome. *Biol Psychiatry* 1992;32:756–765.
  55. Charness ME. Brain lesions in alcoholics. *Alcoholism: Clin Exp Res* 1993;17:2–11.
  56. Folstein SE, Abbott MH, Chase GA, et al. The association of affective disorder with Huntington's disease in a case series and in families. *Psychol Med* 1983;13:537–542.
  57. Starkstein SE, Robinson RG. Affective disorders and cerebral vascular disease. *Br J Psychiatry* 1989;154:170–182.
  58. Burns A, Jacoby R, Levy R. Psychiatric phenomena in Alzheimer's disease. III. Disorders of mood. *Br J Psychiatry* 1990;157:81–86.
  59. Cummings JL. Depression and Parkinson's disease: a review. *Am J Psychiatry* 1992;149:443–454.
  60. Kumar A, Jin Z, Bilker W, et al. Late-onset minor and major depression: early evidence for common neuroanatomic substrates detected by using MRI. *Proc Natl Acad Sci USA* 1998;95:7654–7658.
  61. Coffey CE, Figiel GS, Djang WT, et al. Subcortical hyperintensity on magnetic imaging: a comparison of normal and depressed elderly subjects. *Am J Psychiatry* 1990;147:187–189.
  62. Zubenko GS, Sullivan P, Nelson JP, et al. Brain imaging abnormalities in mental disorders of late life. *Arch Neurol* 1990;47:1107–1111.
  63. Lesser IM, Miller BL, Boone KB, et al. Brain injury and cognitive function in late-onset psychotic depression. *J Neuropsychiatry Clin Neurosci* 1991;3:33–40.
  64. Howard RJ, Beats B, Forstl H, et al. White matter changes in late-onset depression: a magnetic resonance imaging study. *Int J Geriatr Psychiatry* 1993;8:183–185.
  65. Krishnan KR, McDonald WM, Doraiswamy PM. Neuroanatomic substrates of depression in the elderly. *Eur Arch Psychiatry Clin Neurosci* 1993;243:41–46.
  66. Hickie I, Scott E, Mitchell P, et al. Subcortical hyperintensities on magnetic resonance imaging: clinical correlates and prognostic significance in patients with severe depression. *Biol Psychiatry* 1995;37:151–160.
  67. Guze BH, Szuba MP. Leukoencephalopathy and major depression: a preliminary report. *Psychiatry Res* 1992;45:169–175.
  68. Fazekas F, Kleinert R, Offenbacher H, et al. The morphologic correlate of incidental punctate white matter hyperintensities on MR images. *AJNR Am J Neuroradiol* 1991;12:915–921.
  69. Mirsen TR, Lee DH, Wong CJ, et al. Clinical correlates of white-matter changes on magnetic resonance imaging scans of the brain. *Arch Neurol* 1991;48:1015–1021.
  70. Fujikawa T, Yamawaki S, Touhouda Y. Incidence of silent cerebral infarction in patients with major depression. *Stroke* 1993;24:1631–1634.
  71. Fujikawa T, Yamawaki S, Touhouda Y. Background factors and clinical symptoms of major depression with silent cerebral infarction. *Stroke* 1994;25:798–801.
  72. Krishnan KR, Goli V, Ellinwood EH, et al. Leukoencephalopathy in patients diagnosed as major depressive. *Biol Psychiatry* 1988;23:519–522.
  73. Krishnan K, Hays J, Blazer D. MRI-Defined vascular depression. *Am J Psychiatry* 1997;154:497–501.
  74. Strakowski SM, Wilson DR, Tohen M, et al. Structural brain abnormalities in first-episode mania. *Biol Psychiatry* 1993;33:602–609.
  75. Harvey I, Persaud R, Ron MA, et al. Volumetric MRI measurements in bipolars compared with schizophrenics and healthy controls. *Psychol Med* 1994;24:689–699.
  76. Schlaepfer TE, Harris GJ, Tien AY, et al. Decreased regional cortical gray matter volume in schizophrenia. *Am J Psychiatry* 1994;151:842–848.
  77. Pearlson GD, Barta PE, Powers RE, et al. Ziskind-Somerfeld Research Award 1996. Medial and superior temporal gyral volumes and cerebral asymmetry in schizophrenia versus bipolar disorder. *Biol Psychiatry* 1997;41:1–14.
  78. Zipursky RB, Seeman MV, Bury A, et al. Deficits in gray matter volume are present in schizophrenia but not bipolar disorder. *Schizophr Res* 1997;26:85–92.
  79. Young RC, Patel A, Meyers BS, et al. Alpha(1)-acid glycoprotein, age, and sex in mood disorders. *Am J Geriatr Psychiatry* 1999;7:331–334.
  80. Lim KO, Rosenbloom MJ, Faustman WO, et al. Cortical gray matter deficit in patients with bipolar disorder. *Schizophr Res* 1999;40:219–227.
  81. Swayze VW 2d, Andreasen NC, Alliger RJ, et al. Structural brain abnormalities in bipolar affective disorder. Ventricular enlargement and focal signal hyperintensities. *Arch Gen Psychiatry* 1990;47:1054–1059.
  82. McDonald WM, Krishnan KR, Doraiswamy PM, et al. Occurrence of subcortical hyperintensities in elderly subjects with mania. *Psychiatry Res* 1991;40:211–220.
  83. Altshuler LL, Conrad A, Hauser P, et al. Reduction of temporal lobe volume in bipolar disorder: a preliminary report of magnetic resonance imaging. *Arch Gen Psychiatry* 1991;48:482–483.
  84. Johnstone EC, Owens DG, Crow TJ, et al. Temporal lobe structure as determined by nuclear magnetic resonance in schizophrenia and bipolar affective disorder. *J Neurol Neurosurg Psychiatry* 1989;52:736–741.
  85. Altshuler LL, Bartzokis G, Grieder T, et al. Amygdala enlargement in bipolar disorder and hippocampal reduction in schizophrenia: an MRI study demonstrating neuroanatomic specificity. *Arch Gen Psychiatry* 1998;55:663–664.
  86. Coffman JA, Bornstein RA, Olson SC, et al. Cognitive impairment and cerebral structure by MRI in bipolar disorder. *Biol Psychiatry* 1990;27:1188–1196.
  87. Aylward EH, Roberts-Twillie JV, Barta PE, et al. Basal ganglia

- volumes and white matter hyperintensities in patients with bipolar disorder. *Am J Psychiatr* 1994;151:687–693.
88. Strakowski SM, DelBello MP, Sax KW, et al. Brain magnetic resonance imaging of structural abnormalities in bipolar disorder. *Arch Gen Psychiatry* 1999;56(3):254–260.
  89. Hauser P, Altshuler LL, Berrettini W, et al. Temporal lobe measurement in primary affective disorder by magnetic resonance imaging. *J Neuropsychiatry Clin Neurosci* 1989;1:128–134.
  90. Manji HK, Moore GJ, Chen G. Lithium up-regulates the cytoprotective protein Bcl-2 in the CNS in vivo: a role for neurotrophic and neuroprotective effects in manic depressive illness. *J Clin Psychiatry* 2000;61:82–96.
  91. Fujikawa T, Yamawaki S, Touhouda Y. Silent cerebral infarctions in patients with late-onset mania. *Stroke* 1995;26:946–949.
  92. Dupont RM, Jernigan TL, Butters N, et al. Subcortical abnormalities detected in bipolar affective disorder using magnetic resonance imaging. Clinical and neuropsychological significance. *Arch Gen Psychiatry* 1990;47:55–59.
  93. Brown FW, Lewine RJ, Hudgins PA, et al. White matter hyperintensity signals in psychiatric and nonpsychiatric subjects. *Am J Psychiatry* 1999;149:620–625.
  94. Lafer B, Renshaw PF, Sachs G, et al. Proton MRS of the basal ganglia in bipolar disorder. *Biol Psychiatry* 1994;35:685.
  95. Hamakawa H, Kato T, Murashita J, et al. Quantitative proton magnetic resonance spectroscopy of the basal ganglia in patients with affective disorders. *Eur Arch Psychiatry Clin Neurosci* 1998;248:53–58.
  96. Ohara K, Isoda H, Suzuki Y, et al. Proton magnetic resonance spectroscopy of the lenticular nuclei in bipolar I affective disorder. *Psychiatry Res Neuroimag* 1998;84:55–60.
  97. Buchsbaum MS, Wu J, DeLisi LE, et al. Frontal cortex and basal ganglia metabolic rates assessed by positron emission tomography with [<sup>18</sup>F]2-deoxyglucose in affective illness. *J Affect Disord* 1986;10:137–152.
  98. Kishimoto H, Takazu O, Ohno S, et al. 11C-glucose metabolism in manic and depressed patients. *Psychiatry Res* 1987;22:81–88.
  99. Conturo TE, Lori NF, Cull TS, et al. Tracking neuronal fiber pathways in the living human brain. *Proc Natl Acad Sci USA* 1999;96:10422–10427.
  100. Nibuya M, Morinobu S, Duman RS. Regulation of BDNF and trkB mRNA in rat brain by chronic electroconvulsive seizure and antidepressant drug treatments. *J Neurosci* 1995;15:7539–7547.
  101. Nibuya M, Nestler EJ, Duman RS. Chronic antidepressant administration increases the expression of cAMP response element binding protein (CREB) in rat hippocampus. *J Neurosci* 1996;16:2365–2372.
  102. Viadya VA, Duman RS. Role of 5-HT<sub>2A</sub> receptors in down-regulation of BDNF by stress. *Neurosci Lett* 1999;287:1–4.
  103. Watanabe Y, Gould H, Cameron D, et al. Phenytoin prevents stress and corticosterone induced atrophy of CA3 pyramidal neurons. *Hippocampus* 1992;2:431–436.
  104. Duman RS, Malberg JE. Neural plasticity in the pathophysiology and treatment of depression. *Am Coll Neuropsychopharmacol* 1998;37:261.
  105. Jacobs BL, Tanapat P, Reeves AJ, et al. Serotonin stimulates the production of new hippocampal granule neurons via the 5-HT<sub>1A</sub> receptor in the adult rat. *Soc Neurosci* 1998;24:1992.
  106. Duman RS, Heninger GR, Nestler EJ. A molecular and cellular theory of depression. *Arch Gen Psychiatry* 1997;54:597–606.
  107. Raichle ME. Higher function of the brain. In: Bloom F, ed. *Handbook of physiology: Section 1. The nervous system*. Bethesda, MD: American Physiological Society, 1987:643–674.
  108. Sackeim HA, Prohovnik I, Moeller JR, et al. Regional cerebral blood flow in mood disorders. I. Comparison of major depressives and normal controls at rest. *Arch Gen Psychiatry* 1990;47:60–70.
  109. Lesser IM, Mena I, Boone KB, et al. Reduction of cerebral blood flow in older depressed patients. *Arch Gen Psychiatry* 1994;51:677–686.
  110. Baxter LR Jr, Schwartz JM, Phelps ME, et al. Reduction of prefrontal cortex glucose metabolism common to three types of depression. *Arch Gen Psychiatry* 1989;46:243–250.
  111. Dolan RJ, Bench CJ, Liddle PF, et al. Dorsolateral prefrontal cortex dysfunction in the major psychoses: symptom or disease specificity? *J Neurol Neurosurg Psychiatry* 1993;56:1290–1294.
  112. Drevets WC, Videen TO, Price JL, et al. A functional anatomic study of unipolar depression. *J Neurosci* 1992;12:3628–3641.
  113. Bench CJ, Friston KJ, Brown RG, et al. Regional cerebral blood flow in depression measured by positron emission tomography: the relationship with clinical dimensions. *Psychol Med* 1993;23:579–590.
  114. Grasby PM. Imaging strategies in depression. *J Psychopharmacol* 1999;13:346–351.
  115. Fox PT, Mintun MA. Noninvasive functional brain mapping by change-distribution analysis of averaged PET images of H<sub>2</sub>15O tissue activity. *J Nucl Med* 1989;30:141–149.
  116. Friston KJ, Frith CD, Liddle PF, et al. Comparing functional (PET) images: the assessment of significant change. *J Cereb Blood Flow Metab* 1991;11:690–699.
  117. Lane RD, Reiman EM, Ahern GL, et al. Neuroanatomic correlates of happiness, sadness, and disgust. *Am J Psychiatry* 1997;154:926–933.
  118. Reiman EM, Lane RD, Ahern GL, et al. Neuroanatomic correlates of externally and internally generated human emotion. *Am J Psychiatry* 1997;154:918–925.
  119. Whalen PJ, Rauch SL, Etkoff NL, et al. Masked presentations of emotional facial expressions modulate amygdala activity without explicit knowledge. *J Neurosci* 1998;18:411–418.
  120. Beauregard M, Leroux JM, Bergman S, et al. The functional neuroanatomy of major depression: an fMRI study using an emotional activation paradigm. *Neuroreport* 1998;9:3253–3258.
  121. Mayberg HS, Brannan SK, Mahurin RK, et al. Cingulate function in depression: a potential predictor of treatment response. *Neuroreport* 1997;8:1057–1061.
  122. Mayberg HS, Liotti M, Brannan SK, et al. Reciprocal limbic-cortical function and negative mood: converging PET findings in depression and normal sadness. *Am J Psychiatry* 1999;156:675–682.
  123. Mann JJ, Malone KM, Diehl DJ, et al. Demonstration in vivo of reduced serotonin responsiveness in the brain of untreated depressed patients. *Am J Psychiatry* 1996;153:174–182.
  124. Mintun MA, Raichle ME, Kilbourn MR, et al. A quantitative model for the in vivo assessment of drug binding sites with positron emission tomography. *Ann Neurol* 1984;15:217–227.
  125. Koeppe RA, Holthoff VA, Frey KA, et al. Compartmental analysis of [<sup>11</sup>C]flumazenil kinetics for the estimation of ligand transport rate and receptor distribution using positron emission tomography. *J Cereb Blood Flow Metab* 1991;11:735–744.
  126. Frey KA, Holthoff VA, Koeppe RA, et al. Parametric in vivo imaging of benzodiazepine receptor distribution in human brain. *Ann Neurol* 1991;30:663–672.
  127. Mayberg HS, Robinson RG, Wong DF, et al. PET imaging of

- cortical S<sub>2</sub> serotonin receptors after stroke: lateralized changes and relationship to depression. *Am J Psychiatry* 1988;145:937–943.
128. D'haenen H, Bossuyt A, Mertens J, et al. SPECT imaging of serotonin<sub>2</sub> receptors in depression. *Psychiatry Res* 1992;45(4):227–237.
  129. Sadzot B, Lemaire C, Maquet P, et al. Serotonin 5HT<sub>2</sub> receptor imaging in the human brain using positron emission tomography and a new radioligand, [<sup>18</sup>F]altanserin: results in young normal controls. *J Cerebr Blood Flow Metab* 1995;15:787–797.
  130. Blin J, Sette G, Fiorelli M, et al. A method for the in vivo investigation of the serotonergic 5-HT<sub>2</sub> receptors in the human cerebral cortex using positron emission tomography and 18F-labeled setoperone. *J Neurochem* 1990;54:1744–1754.
  131. Lundkvist C, Halldin C, Ginovart N, et al. [<sup>11</sup>C]MDL 100907, a radioligand for selective imaging of 5-HT<sub>2A</sub> receptors with positron emission tomography. *Life Sci* 1996;58:187–192.
  132. Watabe H, Channing MA, Der MG, et al. Kinetic analysis of the 5-HT<sub>2A</sub> ligand [11C]MDL 100,907. *J Cereb Blood Flow Metab* 2000;20:809–909.
  133. Meyer JH, Kapur S, Houle S, et al. Prefrontal cortex 5-HT<sub>2</sub> receptors in depression: an [<sup>18</sup>F]setoperone PET imaging study. *Am J Psychiatry* 1999;156:1029–1034.
  134. Yatham LN, Liddle PF, Shiah IS, et al. Brain serotonin<sub>2</sub> receptors in major depression. A positron emission tomography study. *Arch Gen Psychol* 2000;57:850–858.
  135. Attar-Levy D, Martinot JL, Blin J, et al. The cortical serotonin<sub>2</sub> receptors studied with positron emission tomography and [<sup>18</sup>F]-Septoperone during depressive illness and antidepressant treatment with clomipramine. *Biol Psychiatry* 1999;45:180–186.
  136. Meltzer CC, Price JC, Mathis CA, et al. PET imaging of serotonin type 2A receptors in late-life neuropsychiatric disorders. *Am J Psychiatry* 1999;156:1871–1878.
  137. Mathis CA, Simpson NR, Mahmood K, et al. [<sup>11</sup>C]WAY 100635: a radioligand for imaging 5-HT<sub>1A</sub> receptors with positron emission tomography. *Life Sci* 1994;55:PL403–407.
  138. Pike VW, McCarron JA, Lammertsma AA, et al. Exquisite delineation of 5-HT<sub>1A</sub> receptors in human brain with PET and [<sup>11</sup>C]WAY-100635. *Eur J Pharmacol* 1996;301:R5–R7.
  139. Drevets WC, Frank E, Price JL, et al. PET imaging of serotonin 1A receptor binding in depression. *Biol Psychiatry* 1999;46:1375–1387.
  140. Sargent PA, Kjaer KH, Bench CJ, et al. Brain serotonin 1A receptor binding measured by positron emission tomography with [<sup>11</sup>C]WAY-100635: effects of depression and antidepressant treatment. *Arch Gen Psychiatry* 2000;57:174–180.
  141. Szabo Z, Kao PF, Scheffel U, et al. Positron emission tomography imaging of serotonin transporters in the human brain. *Synapse* 1995;20:37–43.
  142. Parsey RV, Kegeles LS, Hwang DR, et al. In vivo quantification of brain serotonin transporters in humans using [<sup>11</sup>C]McN 5652. *J Nucl Med* 2000;41:1465–1477.
  143. Malison RT, Price LH, Berman R, et al. Reduced brain serotonin transporter by [123I]-2 beta-carbomethoxy-3 beta-(4-iodophenyl) tropane and single photon emission computed tomography. *Biol Psychiatry* 1998;44:1090–1098.
  144. Chugani DC, Muzik O, Chakraborty P, et al. Human brain serotonin synthesis capacity measured in vivo with α-[C-11]methyl-L-tryptophan. *Synapse* 1998;28:33–43.
  145. D'haenen HA, Bossuyt A. Dopamine D2 receptors in depression measured with single photon emission computed tomography. *Biol Psychiatry* 1994;35:128–132.
  146. Ebert D, Feistel H, Loew T, et al. Dopamine and depression. Striatal dopamine D2 receptor SPECT before and after antidepressant therapy. *Psychopharmacol* 1996;126:91–94.
  147. Larisch R, Klimke A, Vosberg H, et al. In vivo evidence for the involvement of dopamine-D2 receptors in striatum and anterior cingulate gyrus in major depression. *Neuroimage* 1997;5:251–260.
  148. Christian BT, Narayanan TK, Shi B, et al. Quantitation of striatal and extrastriatal D-2 dopamine receptors using PET imaging of [(<sup>18</sup>F)]fallypride in nonhuman primates. *Synapse* 2000;38:71–79.
  149. Louie AY, Huber MM, Ahrens ET, et al. In vivo visualization of gene expression using magnetic resonance imaging. *Nat Biotechnol* 2000;18:321–325.